European Journal of Pharmaceutical Sciences 135 (2019) 51–59

Contents lists available at ScienceDirect

European Journal of Pharmaceutical Sciences

journal homepage: www.elsevier.com/locate/ejps

Evaluation of miscibility and polymorphism of synthetic and natural lipids for nanostructured lipid carrier (NLC) formulations by Raman mapping and multivariate curve resolution (MCR)

Hery Mitsutake[a], Lígia N.M. Ribeiro[b], Gustavo H. Rodrigues da Silva[b], Simone R. Castro[b], Eneida de Paula[b], Ronei J. Poppi[a], Márcia C. Breitkreitz[a,*]

[a] Department of Analytical Chemistry, Institute of Chemistry, UNICAMP, Campinas, São Paulo, Brazil
[b] Department of Biochemistry and Tissue Biology, Institute of Biology, University of Campinas, UNICAMP, São Paulo, Brazil

ARTICLE INFO

Keywords:
MCR-ALS
Nanostructured lipid carriers
Natural lipids
Raman mapping

ABSTRACT

Nanostructured lipid carriers (NLC) belong to youngest lipid-based nanocarrier class and they have gained increasing attention over the last ten years. NLCs are composed of a mixture of solid and liquid lipids, which solubilizes the active pharmaceutical ingredient, stabilized by a surfactant. The miscibility of the lipid excipients and structural changes (polymorphism) play an important role in the stability of the formulation and are not easily predicted in the early pharmaceutical development. Even when the excipients are macroscopically miscible, microscopic heterogeneities can result in phase separation during storage, which is only detected after several months of stability studies. In this sense, this work aimed to evaluate the miscibility and the presence of polymorphism in lipid mixtures containing synthetic (cetyl palmitate, Capryol 90®, Dhaykol 6040 LW®, Precirol ATO5® and myristyl myristate) and natural (beeswax, cocoa and shea butters, copaiba, sweet almond, sesame and coconut oils) excipients using Raman mapping and multivariate curve resolution – alternating least squares (MCR-ALS) method. The results were correlated to the macroscopic stability of the formulations. Chemical maps constructed for each excipient allowed the direct comparison among formulations, using standard deviation of the histograms and the Distributional Homogeneity Index (DHI). Lipid mixtures of cetyl palmitate/Capryol®; cetyl palmitate/Dhaykol®; myristyl myristate/Dhaykol® and myristyl myristate/coconut oil presented a single histogram distribution and were stable. The sample with Precirol®/Capryol® was not stable, although the histogram distribution was narrower than the samples with cetyl palmitate, indicating that miscibility was not the factor responsible for the instability. Structural changes before and after melting were identified for cocoa butter and shea butter, but not in the beeswax. Beeswax + copaiba oil sample was very homogenous, without polymorphism and stable over 6 months. Shea butter was also homogeneous and, in spite of the polymorphism, was stable. Formulations with cocoa butter presented a wider histogram distribution and were unstable. This paper showed that, besides the miscibility evaluation, Raman imaging could also identify the polymorphism of the lipids, two major issues in lipid-based formulation development that could help guide the developer understand the stability of the NLC formulations.

1. Introduction

The research on nanostructured lipid carriers (NLC) is recent and has gained attention due to their higher drug upload and stability compared to solid lipid nanoparticles (SLN), from which they derived. Since the core of SLN contains only solid lipid, its highly ordered crystalline arrangement can expel drug over the time. The incorporation of a liquid lipid in the NLC matrix decreases its melting point and inserts defects in the crystal network that increases the amount of drugs that can be incorporated (Müller et al., 2016; Ribeiro et al., 2016).

Recently, natural lipids have been used as an interesting option in the preparation of NLC formulations, due to their safety, wide applicability, abundance, low cost and diversity compared to synthetic lipids (Pinto et al., 2018; Ribeiro et al., 2017). For example, when vegetable oils, blends of triglycerides, fatty acids, antioxidants and other minor compounds are incorporated in cosmetics and pharmaceutical forms, their intrinsic therapeutic effects (e.g. anti-inflammatory activity, loss of water prevention) are extended to them (Pinto et al., 2018). The

* Corresponding author.
E-mail address: marciacb@unicamp.br (M.C. Breitkreitz).

https://doi.org/10.1016/j.ejps.2019.05.002
Received 24 December 2018; Received in revised form 25 March 2019; Accepted 4 May 2019
Available online 06 May 2019

natural excipients based on vegetable butters like cocoa butter (*Theobroma cacao* L.) and shea butter (*Vitellaria paradoxa*) were already approved by the Food and Drug Administration (FDA) as pharmaceutical excipients, being widely used in cosmetic industry (Attama et al., 2006; Hajj Ali et al., 2018).

Solid and liquid lipids, even when macroscopically miscible, may show microscopic heterogeneities that can result in instabilities and phase separation during NLC storage (Rodrigues da Silva et al., 2017). Also, the spatial distribution of excipients in the nanoparticles can influence on the release rate and reproducibility of the process. The discovery of instabilities in early stages of pharmaceutical development represents a time and reagents economy. The miscibility between excipients has been evaluated from the visual observation of the presence or absence of oil droplets on the surface of the mixture between the two lipids (Tichota et al., 2014). However, microscopic immiscibility might not be detected using this method, therefore, our group has been working with the development of methodologies based on Raman mapping for the evaluation of miscibility among semi-solid compounds (Breitkreitz et al., 2013; Rodrigues da Silva et al., 2017; Mitsutake et al., 2018).

Other problems that can affect these formulations are the polymorphic transformations of lipid excipients, directly associated with instability issues (Battaglia and Gallarate, 2012; Kathe et al., 2014; Negi et al., 2014. Negi et al. proposed a protocol to help the selection of lipids for NLC formulations and highlighted that stability issues related to polymorphism of lipids (Negi et al., 2014). Kathe et al. pointed out that the characterization of lipids is a major aspect of study because they can undergo transformation during formulation and can control the system instability (Kathe et al., 2014). The analysis of lipid crystallization tendencies and polymorphic transitions is normally carried out by X-Ray diffractometry, Differential Scanning Calorimetry (DSC) and a less often by single-point Raman spectroscopy (Kathe et al., 2014; Bresson et al., 2011).

Raman spectroscopy is based on inelastic scattering of light, and spectra are shown as the difference between incident and scattered light (Gordon and McGoverin, 2011; Stewart et al., 2012). From the combination of a microscope and a Raman spectrometer, it is possible to obtain chemical and spatial information, giving rise to Raman mapping mode of analysis. In this technique, spectra are acquired by a surface unit of sample called pixel which enables the visualization of spatial distribution of the compounds (de Juan et al., 2004). Thus, it is possible to analyze the homogeneity of formulations once the images are generated based on differences in chemical/physical composition in each pixel. It should be highlighted that the features of single-point Raman spectroscopy in the identification of chemical and physical features of samples are even more pronounced in the mapping mode, due to the larger area mapped.

The simplest data treatment to generate the images is the extraction of information in a single wavenumber, i.e., the univariate method, however due to the strong overlapping of peaks and complexity of signals, the use of chemometric methods is recommended, since they allow the extraction of the information in a multivariate way. One of these methods is the classical least squares (CLS), which is simple and easy to use. In CLS, the score values of each component are calculated by direct regression using pure spectra. However, this is not flexible and only the variability due to concentration is modeled. Considering that in semi-solid formulations there is a higher possibility of interaction between the excipients, the use of the multivariate curve resolution – alternating least squares (MCR-ALS) (de Juan et al., 2014; Zhang et al., 2015) is advisable. The iterative resolution of MCR-ALS takes into account physical and chemical variation sources that could affect the spectral profile of pure compounds in the mixture and therefore it can accommodate the interactions (if present) in the calculations in order to achieve a better fit. Similarly to CLS, MCR-ALS can generate images using a single data set, without the need for a calibration sample set, which makes it adequate in early stages of pharmaceutical development for the choice of the excipients. (de Juan et al., 2014; Gordon and McGoverin, 2011).

The standard deviation of histograms obtained by the images can be used to compare the homogeneity of samples (Mitsutake et al., 2018; Rodrigues da Silva et al., 2017). However, this is a subjective criterion and two maps with same constitutional homogeneity can be spatially totally different. To overcome this problem, the use of Distributional Homogeneity Index (DHI), which is based on macropixels and Continuous-Level Moving Block (CLMB), is indicated (Sacré et al., 2014). DHI does not use a specific calibration model and it can be applied to images generated by any chemometric method.

This work evaluates the miscibility and polymorphism of synthetic (cetyl palmitate, Capryol 90®, Dhaykol 6040 LW®, Precirol ATO5®, myristyl myristate) and natural (beeswax, cocoa and shea butter, copaiba, sweet almond, sesame and coconut oils) mixtures for the NLC preparation using Raman mapping and MCR-ALS trying to associate the results with the observed macroscopic stability of the complete NLC formulations. STD and DHI were used to evaluate the miscibility. This work is intended to show the use of this methodology for the pre-formulation stage, as a first screening of different excipients, prior to formulation development.

2. Materials and methods

2.1. Materials

Cetyl Palmitate and Dhaykol 6040® were purchased from Dhaymers Química Fina (Brazil), Capryol 90® and Precirol ATO5® were obtained by Gattefossé (France). Myristyl myristate was purchased from Croda (Brazil). Beeswax (from *Apis mellifera*), shea and cocoa butter, copaiba,

Table 1
Chemical composition of the excipients used in this study.

Name	Chemical compound(s)
Cetyl palmitate	Hexadecyl hexadecanoate
Dhaykol 6040 LW®	Decanoic acid/octanoic acid
Capryol 90®	Propylene glycol esters of caprylic acid
Precirol ATO5®	Esters of palmitic and stearic acids
Myristyl myristate	Tetradecyl tetradecanoate
Beeswax	C27-C33 hydrocarbons; C24-C32 free fatty acids; C28-C35 free fatty alcohols; C40-C48 linear wax monoesters and hydroxymonoesters; complex wax esters (Fratini et al., 2016)
Shea butter	Oleic, stearic, linoleic and palmitic acids; unsaponifiable material, triterpene, tocopherol, phenols and sterols (Honfo et al., 2014)
Cocoa butter	Palmitic, stearic, oleic and linoleic acids (Servent et al., 2018)
Copaiba oil	Saturated fatty acids (capric, caprylic, behenic, lignoceric, lauric, palmitic acid), linoleic and arachidonic acid, sesquiterpenes, diterpenes, β-caryophyllene (Dias et al., 2014)
Sweet almond oil	Unsaturated fatty acids mainly linoleic (~65%), and palmitic acids, β-sitosterol, α- and γ-tocopherol (Fernandes et al., 2017)
Sesame oil	Oleic and linoleic acids, tocopherol and sesamolin (Hashempour-Baltork et al., 2018)
Coconut oil	Saturated fatty acids (trilaurin, palmitic acids), oleic acid (Bezard et al., 1971)

Table 2
Composition of the pre-formulation mixtures.

	Solid lipid	Liquid lipid	Solid concentration (% w/w)	Liquid concentration (% w/w)
Synthetic solid excipients	Cetyl palmitate	Capryol 90®	70.0	30.0
	Cetyl palmitate	Dhaykol 6040 LW®	70.0	30.0
	Precirol ATO5®	Capryol 90®	83.3	16.7
	Myristyl myristate	Dhaykol 6040 LW®	70.0	30.0
	Myristyl myristate	Coconut oil	79.7	20.3
Natural solid excipients	Beeswax	Copaiba oil	81.5	18.5
	Cocoa butter	Coconut oil	75.0	25.0
	Cocoa butter	Sesame oil	75.0	25.0
	Shea butter	Sweet almond oil	75.0	25.0

sweet almond, sesame and coconut oil were provided by Engetec Engineering (Brazil). Table 1 shows the main chemical compounds found in each excipient tested.

2.2. Sample preparation

The samples were prepared by heating (10 °C above the melting point of the solid lipid); the liquid excipients were added under stirring until a visually homogeneous mixture was obtained. The composition of each sample is shown in Table 2 where the major component was the solid lipid (70.0–83.3% w/w) and the concentration of liquid lipid varied from 16.7 to 30.0%, w/w.

2.3. Raman mapping

The samples were cooled to room temperature in an aluminum cell and an area of 2.0 × 2.0 mm (4 mm^2) was mapped using a Raman Station 400 (Perkin Elmer, CT, USA). A laser of 785 nm was used as an excitation light, with nominal power of 100 mW.

The exposure time was 3 s/pixel and each spectrum was the average of 2 exposures. The pixel size was 50 µm, spectral range of 600–3200 cm^{-1} with resolution of 4 cm^{-1}. Each sample generated a cube of data with dimensions of 40 × 40 × 651, where 40 was number of pixels at *x* and *y* axis and 651 the number of spectral variables.

The spectra of vegetable butters were obtained before and after their melting, in the latter case after solidification at room temperature (25 °C).

2.4. Chemometric analysis

2.4.1. Data processing

Spikes from Raman spectra were excluded using the algorithm developed by Sabin and co-workers (Sabin et al., 2012). The data cube was unfolded to a 2D matrix NM × λ, where M is number of pixels at *x* axis, N is the number of pixels at *y* axis and λ is the number of spectral variables. The spectra were smoothed using Savitzky-Golay (width of 5, second polynomial order), baseline correction by asymmetric least squares or weighted least squares and normalization using unit vector. The spectral range chosen to build the models was 1804–724 cm^{-1}.

2.4.2. Multivariate curve resolution – alternating least squares (MCR-ALS)

MCR method is based on the bilinear model shown in Eq. (1):

$$\boldsymbol{D} = \boldsymbol{CS}^{\boldsymbol{T}} + \boldsymbol{E} \quad (1)$$

where **D** ($NM \times \lambda$) is 2D matrix with sample spectra, **C** ($NM \times A$) contains the concentration profiles, $\mathbf{S}^{\mathrm{T}}$ ($A \times \lambda$) contain the pure spectral profile and **E** is the matrix with variance unexplained by model for A factors used in chemometric model. The aim of this method is to solve the mixture problem (de Juan et al., 2014), providing a chemically meaningful additive bilinear model of the pure contributions, i.e., concentrations and spectral profile. Eq. (1) can be reorganized in Eqs. (2) and (3):

$$\boldsymbol{C} = \boldsymbol{DS}(\boldsymbol{S}^{\boldsymbol{T}}\boldsymbol{S})^{-1} \quad (2)$$

$$\boldsymbol{S}^{T} = (\boldsymbol{C}^{T}\boldsymbol{C})^{-1}\boldsymbol{C}^{T}\boldsymbol{D} \quad (3)$$

MCR requires an initial estimative of **C** or $\mathbf{S}^{\mathrm{T}}$, to initialize the calculations. One of the most used algorithms is alternating least squares (ALS) that iteratively optimize the recovers of **C** and $\mathbf{S}^{\mathrm{T}}$ matrix. In this work, the number of factors was chosen using singular value decomposition (SVD) and we used augmented matrix with pure excipient spectra. SIMPLISMA (SIMPLe-to-use Interactive Self-modeling Mixture Analysis) algorithm was employed to provide initial estimative of $\mathbf{S}^{\mathrm{T}}$ and non-negativity in concentration and spectral profiles were the constraints applied (de Juan et al., 2014). In the samples containing vegetable butters, pure excipient spectra were used as initial estimative, due to the high spectral similarities between the two polymorphic forms. In the cases where baseline was corrected by weighted least squares only non-negativity in the concentration was applied. The models were built using Matlab version 8.3 (Mathworks Inc., Natick MA, USA) and MCR_gui version 2.

2.4.3. Distributional Homogeneity Index – DHI

Refolding the MCR-ALS scores, the chemical maps of distribution of the excipients were generated. From these maps, the DHI was calculated for each of the excipients. In the DHI calculations, first the distribution map is sampled by all possible macropixel of 2 × 2 original pixel size. This step is repeated using size 3 × 3, 4 × 4 successively until unit macropixel size. For each macropixel size, the standard deviation is calculated and plotted against the macropixel size, obtaining homogeneity curve. Then the map is randomized and the homogeneity curve of the random map is computed. DHI value is obtained by the ratio of the area under the homogeneity curve (AUC) of the studied map and the area under the homogeneity curve of the randomized map (Sacré et al., 2014). DHI values increases as the homogeneity of the distribution map decreases. The DHI algorithm was kindly provided by Pierre-Yves Sacré (University of Liège, Belgium) and calculations were carried out using Matlab version 8.3.

3. Results and discussion

Raman spectra of all excipients (except vegetable butters, which will be discussed further on) are shown in Fig. 1. Due to the similar chemical composition of solid excipients, their Raman spectra are very similar. Peak at 1440 cm^{-1} is related to -CH_2 bonds (Patnaik, 2004) while the peaks at 1132 and 1064 cm^{-1} refer to C—C asymmetric and symmetric stretching, respectively. Peak assigned to the C═O bonds of COOH groups can be seen at 1420 cm^{-1} (Zhao et al., 2004) for all samples, except Precirol ATO5®. Peaks at 1296 cm^{-1} are attributed to CH_2 twisting and between 800 and 900 cm^{-1} to CH_3 rocking (Saupe et al., 2006). In liquid excipients, weak peaks from 1736 to 1748 cm^{-1} are related to the carbonyl bond ν-(C = O). The peak at 1656 cm^{-1}, present only in sweet almond and copaiba oils, is associated with *cis* RCH = CHR of olefinic molecules and appears associated with degree of unsaturation of these oils. Bands around 1300 cm^{-1} are related with methylene

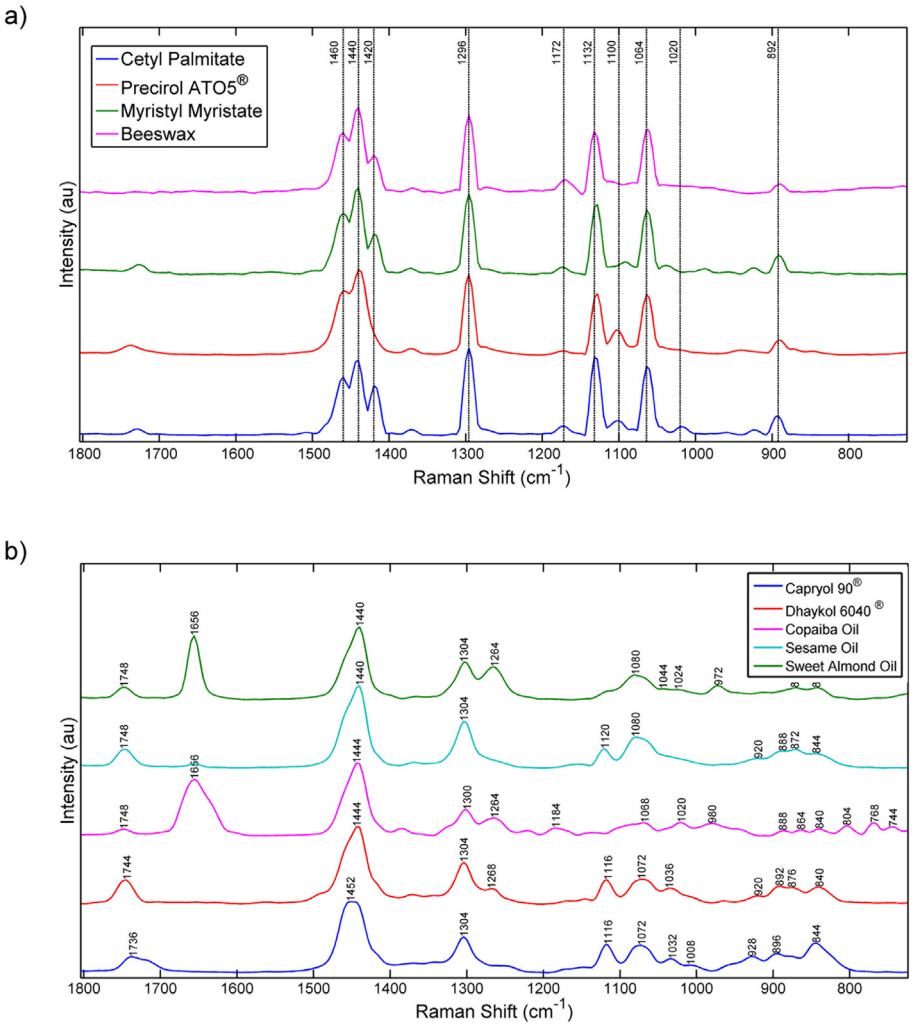

Fig. 1. Raman spectra of a) solid and b) liquid excipients.

twisting deformation vibration. Bands 1100–100 and 900–800 cm^{-1} are related with $-(CH_2)_n-$ stretching on liquid excipients (Baeten et al., 1998).

3.1. Pre-formulations with synthetic solid excipients

Table 3 shows the parameters of MCR-ALS, and correlation coefficients between the real spectra and the recovered profile for the synthetic excipients. Lack of fit represents the dissimilarity between the experimental data matrix (**D**) and the product ($\mathbf{CS}^T$), calculated by MCR-ALS (de Juan et al., 2014). This is one figure of merit of the MCR-ALS optimization procedure and it is very useful to evaluate and understand if the experimental data are well fit to the model (Jaumot et al., 2005). Assessing the lack of fit (maximum of 0.8923% by principal component analysis, PCA) and percentage of explained variance (minimum of 99.5928%), the models built for these five formulations can be considered well adjusted. In other words, the difference between experimental data (**D**, the Raman spectra) and $\mathbf{CS}^T$ (MCR-ALS parameters) is very low and therefore the calculated concentrations can be used to build chemical maps of these excipients. The correlation coefficients between original and recovered spectra are used to attribute each map to a specific compound. The coefficients are higher than 0.9842 indicating excellent spectra recovering. Fig. 2 compares $\mathbf{S}^T$ and original Raman spectra of cetyl palmitate/Capryol 90® sample, showing no indication of rotational ambiguity. In other words, the peaks of cetyl palmitate are not present in Capryol 90® recovered spectrum and vice-versa. The same results were obtained for the other samples.

Fig. 3 shows chemical maps and histograms of pixel distribution of formulations using cetyl palmitate. The closer to the red color the higher the concentration of a given excipient. Another important

Table 3
MCR-ALS results for the pre-formulations developed using synthetic excipients.

Pre formulation	Number of factors	Lack of fit (% PCA)	Explained variance (%)	Correlation coefficient - solid lipid	Correlation coefficient - liquid lipid
Cetyl palmitate/Capryol®	2	0.8923	99.6185	0.9941	0.9777
Cetyl palmitate/Dhaykol 6040 LW®	2	0.4297	99.6638	0.9956	0.9835
Precirol®/Capryol®	2	0.1218	99.8972	0.9924	0.9998
Myristyl myristate/Dhaykol 6040 LW®	2	0.0835	99.5928	0.9845	0.9842
Myristyl myristate/coconut oil	2	0.0934	99.6505	0.9947	0.9993

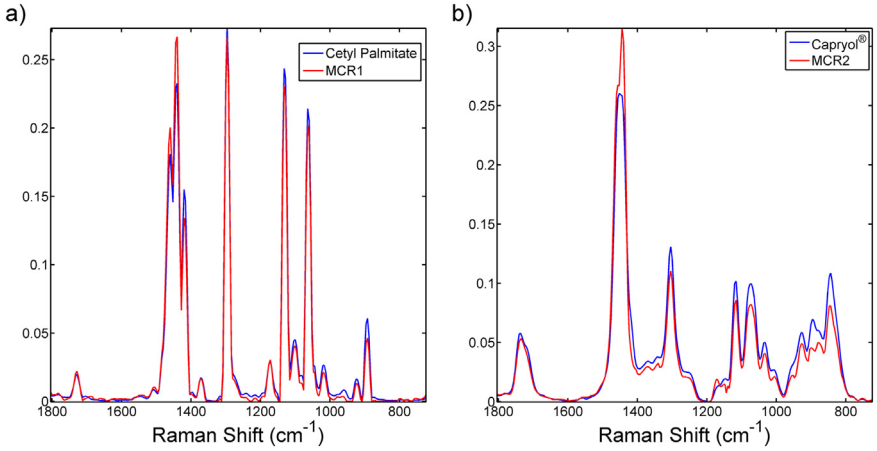

Fig. 2. Original and recovered spectra for cetyl palmitate/Capryol® sample: a) cetyl palmitate and b) Capryol®.

parameter is the map complementarity: in regions where there is more of the first excipient, it is necessary to find less of the second, so that the histograms should resemble a mirror image of one another. Also, as scores of MCR-ALS (**C**) varies between 0 to 1, it is possible to do a direct comparison of samples with different excipients. To facilitate the comparison, **C** were multiplied by 100 and it is shown as percentages. Using standard deviation of histograms (STD) and DHI it was possible to evaluate and compare the miscibility of different formulations. We must highlight that the values in **C** are *related* to the concentrations, but they are not the real concentration values of the excipients – therefore the mean value should not be compared to the real concentration of each excipient. If it is necessary to obtain the real concentration values, it is mandatory the use of a calibration model (e.g., Partial Least Squares, PLS) or MCR-ALS with the correlation constraint in, both requiring a calibration sample set to be prepared. However, the aim of this work is to do a comparison of pre-formulations of several excipients using a methodology that does not require a calibration sample set, only the pure spectra of the constituents. Using these maps, is verified that cetyl palmitate presented a good miscibility with Capryol® and Dhaykol 6040 LW® (maximum STD of 6.8 and DHI of 6.0). In a previous work (Mitsutake et al., 2018), we have shown that Transcutol® has a poor miscibility with cetyl palmitate, with two populations in the histogram and phase separation after 60 days, differently of what was observed for Capryol® and Dhaykol 6040 LW® These results highlight the potential of this technique to predict stability problems during pharmaceutical development.

The maps of the mixtures Precirol®/Capryol®, myristyl myristate/Dhaykol 6040 LW® and myristyl myristate/coconut oil are shown in Fig. 4. The first showed the highest homogeneity with a STD of 1.4 and 1.6 for solid and liquid excipients, respectively. Nevertheless, it was observed that this sample presented stability problems over the time. Precirol® is an excipient known by having an aging effect, a possible source of this stability problem (Hamdani et al., 2003). This outcome shows that the instability of this lipid mixture is not associated with the miscibility of the compounds and highlights the importance of following changes over the time to identify aging effects. The myristyl myristate and Dhaykol 6040® have a STD of 8.2 and 9.2 respectively. The mixture of myristyl myristate and coconut oil was more homogeneous, with STD of 2.7 and 3.0, respectively. In the case of these formulations it is interesting to note that DHI results were different compared to STD: the lowest DHI (i.e., the most homogeneous the mixture) was myristyl myristate with coconut oil instead of Precirol ATO5® with Capryol 90®. On the other hand, the formulation of Precirol ATO5® with Capryol 90®, which has a low STD, presented a DHI of 5.8 and 5.7. This is due to the small cluster found in the image, which generated a tail and decreased the asymmetry of the histograms (Fig. 4a). The samples with myristyl myristate were observed to be stable, without phase separation. Table 4 shows the DHI and STD obtained from pre-formulations using synthetic solid excipients.

3.2. Pre-formulations with natural solid excipients

In addition to formulations developed using synthetic excipients, we also analyzed systems containing only natural lipids: beeswax, two vegetable butters (cocoa and shea) and 4 vegetable oils (coconut, sesame, copaiba and sweet almond oil). The lack of fit, percentage of explained variance and correlation coefficients with original spectra are shown in Table 5. The most homogenous formulation was obtained using beeswax and copaiba oil as excipients (maximum STD of 0.7 and DHI of 2.7) and it did not present stability issues or polymorphism in the period of 6 months.

On the other hand, polymorphism was identified in cocoa and shea butter, which can be seen by the differences of Raman spectra before and after melting theses butters (Fig. 5). The differences are mainly in the region of 1200–1000 cm^{-1} associated with C—C skeletal modes. Peaks around 1128 and 1060 cm^{-1} can be associated with symmetric and antisymmetric C—C stretching, respectively. The peak at 1096 cm^{-1} is characteristic of conformationally disordered alkyl chains

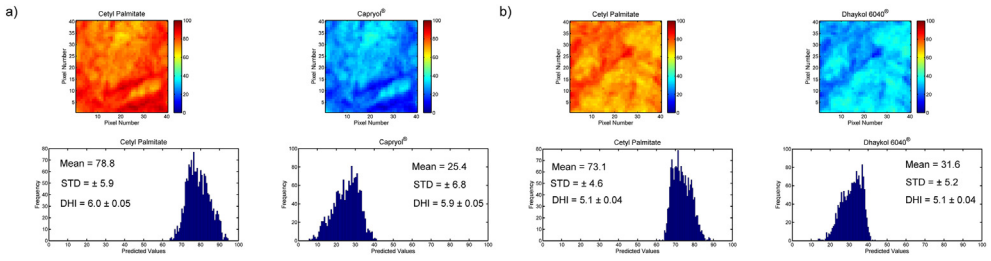

Fig. 3. Chemical maps of cetyl palmitate and: a) Capryol® and b) Dhaykol 6040 LW®. (For interpretation of the references to color in this figure, the reader is referred to the web version of this article.)

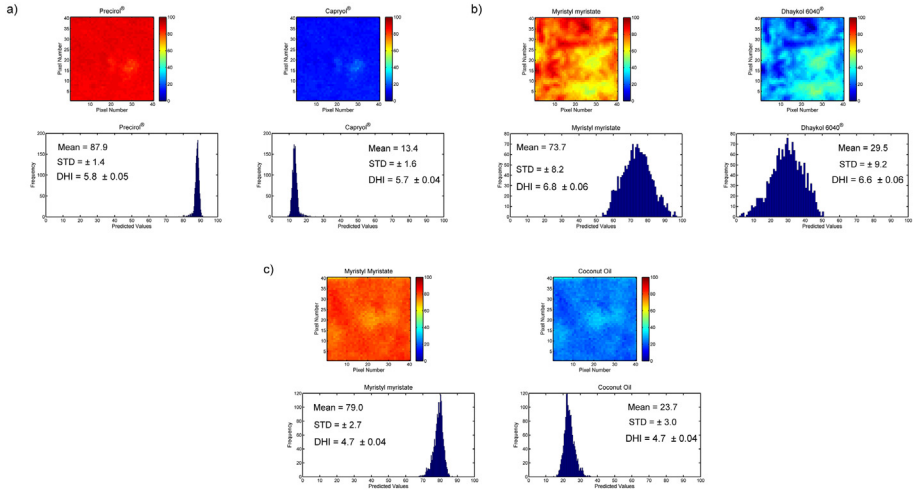

Fig. 4. Chemical maps of: a) Precirol®/Capryol®, b) myristyl myristate/Dhaykol 6040 LW® and c) myristyl myristate/coconut oil.

Table 4
DHI and STD obtained for pre-formulations using synthetic solid excipients.

Sample	DHI (solid)	STD (solid)	DHI (liquid)	STD (liquid)
Cetyl palmitate/Capryol 90®	6.0 ± 0.05	5.9	5.9 ± 0.05	5.2
Cetyl palmitate/Dhaykol 6040 LW®	5.1 ± 0.04	4.6	5.1 ± 0.04	5.2
Precirol ATO5®/Capryol 90®	5.8 ± 0.05	1.4	5.7 ± 0.04	1.6
Myristyl myristate/Dhaykol 6040 LW®	6.8 ± 0.06	8.2	6.6 ± 0.06	9.2
Myristyl myristate/coconut oil	4.7 ± 0.04	2.7	4.7 ± 0.04	3.0

Table 5
MCR-ALS results for formulations developed using natural excipients.

Pre formulation	Number of factors	Lack of fit (%, PCA)	Explained variance (%)	Correlation coefficient with solid lipid	Correlation coefficient with liquid lipid
Beeswax/copaiba oil	2	0.0003	99.5448	0.9843	0.9949
Cocoa butter/coconut oil	4	0.0095	99.1094	0.9797[a] 0.9869[b]	0.9935
Cocoa butter/sesame oil	3	0.0337	98.9554	0.9884[a] 0.9722[b]	0.9675
Shea butter/sweet almond oil	3	0.0156	99.6803	0.9788[a] 0.9956[b]	0.9950

[a] Form observed before melting the butter.
[b] Form observed after melting of butter.

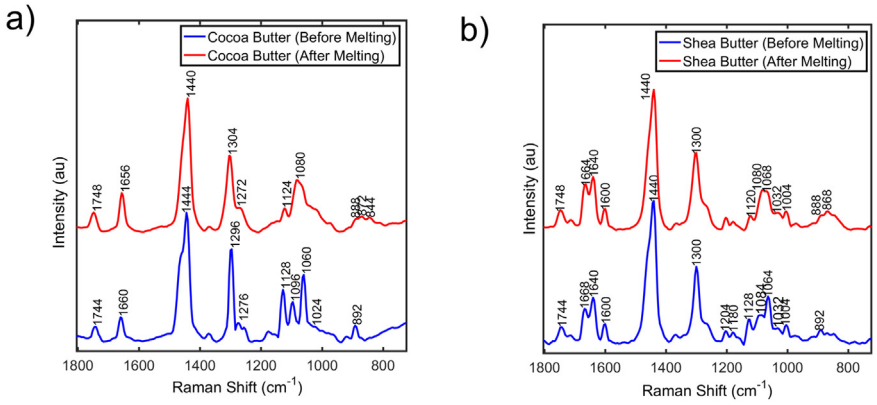

Fig. 5. Raman spectra of a) cocoa and b) shea butter before and after the melting of the butters.

with gauche defects (Bresson et al., 2011). Peaks around 1440 cm^{-1} in liquid excipients (Fig. 1b) and cocoa butter (Fig. 5) can be associated with C—H deformation vibration and unsaturation (Baeten et al., 1998; Bresson et al., 2011). Comparing to the literature, the cocoa butter spectrum of form before and after refers to polymorph 1 and 6, respectively (Bresson et al., 2011; Ribeiro et al., 2017). Because of the polymorphic change, the matrix was augmented using spectra of the vegetable oil and these two forms of the butters. MCR-ALS results for

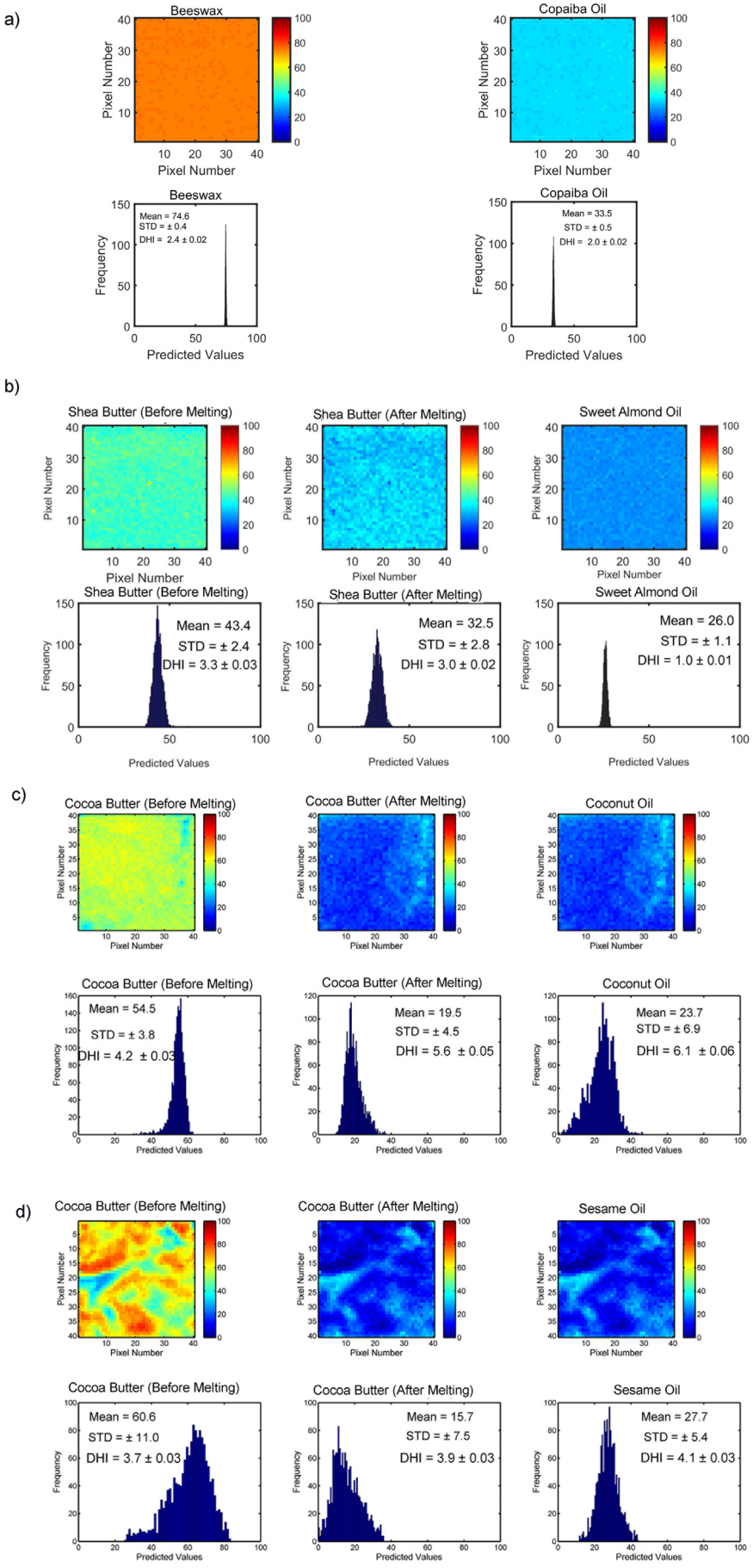

Fig. 6. Chemical maps of formulations: a) beeswax/copaiba oil; b) shea butter/sweet almond oil; c) cocoa butter/coconut oil; d) cocoa butter/sesame oil.

Table 6
DHI and STD obtained for pre-formulations using natural solid excipients.

Sample	DHI (solid)	STD (solid)	DHI (liquid)	STD (liquid)
Beeswax/copaiba oil	2.4 ± 0.02	0.4	2.0 ± 0.02	0.5
Shea butter/sweet almond oil	3.3 ± 0.03[a]	2.4[a]	1.0 ± 0.01	1.1
	3.0 ± 0.02[b]	2.8[b]		
Cocoa butter/coconut oil	4.2 ± 0.03[a]	3.8[a]	6.1 ± 0.06	6.9
	5.6 ± 0.05[b]	4.5[b]		
Cocoa butter/sesame oil	3.7 ± 0.03[a]	11.0[a]	4.1 ± 0.03	5.4
	3.9 ± 0.03[b]	7.5[b]		

[a] Form before melting.
[b] Form after melting.

the pre-formulations developed using natural excipients and this approach are shown in Table 5. All the models were well adjusted, with maximum lack of fit (%) of 0.1201 and minimum explained variance of 98.9554. Even in case of high similarity of Raman spectra, as observed before and after melting forms of butters, spectra were well recovered with minimum correlation coefficient of 0.9675.

The chemical maps obtained for formulations using natural solid excipients are shown in Fig. 6. The most homogeneous sample was beeswax with copaiba oil with STD of 0.4 and 0.5, and DHI of 2.4 and 2.0 for solid and liquid excipients, respectively. These histograms are very narrow and do not present agglomerates in the chemical images, therefore DHI values are the lowest of all samples (Fig. 6a). Among the vegetable butters, the only stable formulation was shea butter/sweet almond oil, the most homogeneous among the butters This sample has STD maximum of 2.8 and DHI maximum of 3.3 (Fig. 6b). Cocoa butter/coconut oil presented an intermediate miscibility (maximum STD and DHI of 6.9 and 6.1, respectively). Cocoa butter/sesame oil presented the poorest miscibility (maximum STD of 11.0, although DHI maximum was 4.1). For this formulation, the form before melting of cocoa butter seems to have lower miscibility with sesame oil. From these results, it can be concluded that polymorphism can be an important source of instability, because even samples with intermediate homogeneity presented macroscopic stability problems (cocoa butter/coconut oil and cocoa butter/sesame oil) in the presence of polymorphism.

A comparison of DHI values and STD for pre-formulations developed using natural solid excipients is presented in Table 6. The samples with beeswax and shea butter, extremely homogeneous, showed the lowest DHI values.

It should be noted that due to differences of predicted ($\mathbf{C}^*\mathbf{S}^T$) and experimental values ($\mathbf{D}$), the values varied between 97.7 and 104.7. One solution to force to 100 is the use of closure constraint, which is a mass-balance constraint. However, the use of this constraint is not advisable in spectroscopic data, it is mainly applied to systems involving chemical reactions (de Juan et al., 2014).

The differences between STD and DHI observed for some pre-formulations are more relevant in cases where small agglomerates appeared, which generated longer tails in the histograms, decreasing their symmetry. DHI is more sensible to alterations on histogram shape than STD because kurtosis is also taken into consideration.

4. Conclusions

This paper showed that, besides the miscibility evaluation, Raman imaging could also identify polymorphism in solid lipids, two major issues in lipid-based formulation development. Due to the fact that samples are mainly composed of triglycerides, their Raman spectra show many overlapped peaks that precludes the use of the univariate method to extract information and generate chemical images. MCR-ALS method was able to recover the lipid excipient spectra with high correlation to the real spectra and generated chemical maps for each compound, which allowed direct comparison among formulations prepared with different excipients. Samples with poor microscopic miscibility of excipients (heterogeneous samples) showed macroscopic phase separation over the time, therefore indicating that Raman imaging could be a useful tool for the screening of excipients during an early stage of the formulation development. However, homogeneous samples also presented stability issues, which can be explained based on other factors, such as polymorphism (as identified in vegetable butters) and aging effect (known for Precirol®).

Declaration of interest

The authors declare they have no conflict of interest.

Acknowledgments

The authors thank INCT-Bioanalítica (FAPESP/INCT 14/50867-3; CNPq/INCT 465389/2014-7), CNPq (H.M. scholarship) and CAPES (Finance Code 001) for financial support; Gattefossé (France) for the donation of Capryol 90® and Precirol ATO5® and Pierre-Yves Sacré (University of Liège, Belgium) for the MATLAB code and helpful discussions about DHI.

References

Attama, A.A., Schicke, B.C., Müller-Goymann, C.C., 2006. Further characterization of theobroma oil – beeswax admixtures as lipid matrices for improved drug delivery systems. Eur. J. Pharm. Biopharm. 64, 294–306. https://doi.org/10.1016/j.ejpb.2006.06.010.

Baeten, V., Hourant, P., Morales, M.T., Aparicio, R., 1998. Oil and fat classification by FT-Raman spectroscopy. J. Agric. Food Chem. 46, 2638–2646. https://doi.org/10.1021/jf9707851.

Battaglia, L., Gallarate, M., 2012. Lipid nanoparticles: state of the art, new preparation methods and challenges in drug delivery. Expert Opin. Drug Deliv. (5), 497–508. https://doi.org/10.1517/17425247.2012.673278.

Bezard, J., Bugaut, M., Clement, G., 1971. Triglyceride composition of coconut oil. J. Am. Oil Chem. Soc. 48, 134–139. https://doi.org/10.1007/BF02545736.

Breitkreitz, M.C., Sabin, G.P., Polla, G., Poppi, R.J., 2013. Characterization of semi-solid Self-Emulsifying Drug Delivery Systems (SEDDS) of atorvastatin calcium by Raman image spectroscopy and chemometrics. J. Pharm. Biomed. Anal. 73, 3–12. https://doi.org/10.1016/j.jpba.2012.03.054.

Bresson, S., Rousseau, D., Ghosh, S., El Marssi, M., Faivre, V., 2011. Raman spectroscopy of the polymorphic forms and liquid state of cocoa butter. Eur. J. Lipid Sci. Technol. 113, 992–1004. https://doi.org/10.1002/ejlt.201100088.

de Juan, A., Tauler, R., Dyson, R., Marcolli, C., Rault, M., Maeder, M., 2004. Spectroscopic imaging and chemometrics: a powerful combination for global and local sample analysis. TrAC Trends Anal. Chem. 23, 70–79. https://doi.org/10.1016/S0165-9936(04)00101-3.

de Juan, A., Jaumot, J., Tauler, R., 2014. Multivariate curve resolution (MCR). Solving the mixture analysis problem. Anal. Methods 6, 4964–4976. https://doi.org/10.1039/c4ay00571f.

Dias, D.O., Colombo, M., Kelmann, R.G., Kaiser, S., Lucca, L.G., Teixeira, H.F., Limberger, R.P., Veiga Jr., V.F., Koester, L.S., 2014. Optimization of copaiba oil-based nanoemulsions obtained by different preparation methods. Ind. Crop. Prod. 59, 154–162. https://doi.org/10.1016/j.indcrop.2014.05.007.

Fernandes, G.D., Gómez-Coca, R.B., Pérez-Camino, M.D.C., Moreda, W., Barrera-Arellano, D., 2017. Chemical characterization of major and minor compounds of nut oils: almond, hazelnut, and pecan nut. J. Chem. 2017, 1–11. https://doi.org/10.1155/2017/2609549.

Fratini, F., Cilia, G., Turchi, B., Felicioli, A., 2016. Beeswax: a minireview of its antimicrobial activity and its application in medicine. Asian Pac J Trop Med 9, 839–843. https://doi.org/10.1016/j.apjtm.2016.07.003.

Gordon, K.C., McGoverin, C.M., 2011. Raman mapping of pharmaceuticals. Int. J. Pharm. 417, 151–162. https://doi.org/10.1016/j.ijpharm.2010.12.030.
Hajj Ali, H., Michaux, F., Khanji, A.N., Jasniewski, J., Linder, M., 2018. Chitosan - shea butter solid nanoparticles assemblies for the preparation of a novel nanoparticles in microparticles system containing curcumin. Colloids Surf. A Physicochem. Eng. Asp. 553, 359–367. https://doi.org/10.1016/j.colsurfa.2018.05.075.
Hamdani, J., Moës, A.J., Amighi, K., 2003. Physical and thermal characterisation of Precirol® and Compritol® as lipophilic glycerides used for the preparation of controlled-release matrix pellets. Int. J. Pharm. 260, 47–57. https://doi.org/10.1016/S0378-5173(03)00229-1.
Hashempour-Baltork, F., Torbati, M., Azadmard-Damirchi, S., Peter Savage, G., 2018. Chemical, rheological and nutritional characteristics of sesame and olive oils blended with linseed oil. Adv. Pharm. Bull. 8, 107–113. https://doi.org/10.15171/apb.2018.013.
Honfo, F.G., Akissoe, N., Linnemann, A.R., Soumanou, M., Van Boekel, M.A.J.S., 2014. Nutritional composition of shea products and chemical properties of shea butter: a review. Crit. Rev. Food Sci. Nutr. (5), 673–686. https://doi.org/10.1080/10408398.2011.604142.
Jaumot, J., Gargallo, R., de Juan, A., Tauler, R., 2005. A graphical user-friendly interface for MCR-ALS: a new tool for multivariate curve resolution in MATLAB. Chemom. Intell. Lab. Syst. 76, 101–110. https://doi.org/10.1016/j.chemolab.2004.12.007.
Kathe, N., Henriksen, B., Chauhan, H., 2014. Physicochemical characterization techniques for solid lipid nanoparticles: principles and limitations. Drug Dev. Ind. Pharm. (12), 1565–1575. https://doi.org/10.3109/03639045.2014.909840.
Mitsutake, H., Castro, S.R., de Paula, E., Poppi, R.J., Rutledge, D.N., Breitkreitz, M.C., 2018. Comparison of different chemometric methods to extract chemical and physical information from Raman images of homogeneous and heterogeneous semi-solid pharmaceutical formulations. Int. J. Pharm. 552, 119–129. https://doi.org/10.1016/j.ijpharm.2018.09.058.
Müller, R.H., Alexiev, U., Sinambela, P., Keck, C.M., 2016. Nanostructured lipid carriers (NLC): the second generation of solid lipid nanoparticles, 2016. In: Percutaneous Penetration Enhancers Chemical Methods in Penetration Enhancement. Chapter 11, pp. 161–185.
Negi, L.M., Jaggi, M., Talegaonkar, S., 2014. Development of protocol for screening the formulation components and the assessment of common quality problems of nanostructured lipid carriers. Int. J. Pharm. 461, 403–410. https://doi.org/10.1016/j.ijpharm.2013.12.006.
Patnaik, P., 2004. Infrared and Raman spectroscopy. In: Dean's Analytical Chemistry Handbook, 2 ed. McGraw-Hill Education.
Pinto, F., de Barros, D.P.C., Fonseca, L.P., 2018. Design of multifunctional nanostructured lipid carriers enriched with α-tocopherol using vegetable oils. Ind. Crop. Prod. 118, 149–159. https://doi.org/10.1016/j.indcrop.2018.03.042.
Ribeiro, L.N.M., Franz-Montan, M., Breitkreitz, M.C., Alcântara, A.C.S., Castro, S.R., Guilherme, V.A., Barbosa, R.M., de Paula, E., 2016. Nanostructured lipid carriers as robust systems for topical lidocaine-prilocaine release in dentistry. Eu. J. Pharm. Sci. 93, 192–202. https://doi.org/10.1016/j.ejps.2016.08.030.
Ribeiro, L.N.M., Breitkreitz, M.C., Guilherme, V.A., da Silva, G.H.R., Couto, V.M., Castro, S.R., de Paula, B.O., Machado, D., de Paula, E., 2017. Natural lipids-based NLC containing lidocaine: from pre-formulation to in vivo studies. Eur. J. Pharm. Sci. 106, 102–112. https://doi.org/10.1016/j.ejps.2017.05.060.
Rodrigues da Silva, G.H., Ribeiro, L.N.M., Mitsutake, H., Guilherme, V.A., Castro, S.R., Poppi, R.J., Breitkreitz, M.C., de Paula, E., 2017. Optimised NLC: a nanotechnological approach to improve the anaesthetic effect of bupivacaine. Int. J. Pharm. 529, 253–263. https://doi.org/10.1016/j.ijpharm.2017.06.066.
Sabin, G.P., de Souza, A.M., Breitkreitz, M.C., Poppi, R.J., 2012. Desenvolvimento de um algoritmo para identificação e correção de spikes em espectroscopia Raman de imagem. Quim Nova 35, 612–615. https://doi.org/10.1590/S0100-40422012000300030.
Sacré, P.-Y., Lebrun, P., Chavez, P.-F., de Bleye, C., Netchacovitch, L., Rozet, E., Klinkenberg, R., Streel, B., Hubert, P., Ziemons, E., 2014. A new criterion to assess distributional homogeneity in hyperspectral images of solid pharmaceutical dosage forms. Anal. Chim. Acta 818, 7−14. https://doi.org/10.1016/j.aca.2014.02.014.
Saupe, A., Gordon, K.C., Rades, T., 2006. Structural investigations on nanoemulsions, solid lipid nanoparticles and nanostructured lipid carriers by cryo-field emission scanning electron microscopy and Raman spectroscopy. Int. J. Pharm. 314, 56–62. https://doi.org/10.1016/j.ijpharm.2006.01.022.
Servent, A., Boulanger, R., Davrieux, F., Pinot, M.-N., Tardan, E., Forestier-Chiron, N., Hue, C., 2018. Assessment of cocoa (*Theobroma cacao* L.) butter content and composition throughout fermentations. Food Res. Int. 107, 675–682. https://doi.org/10.1016/j.foodres.2018.02.070.
Stewart, S., Priore, R.J., Nelson, M.P., Treado, P.J., 2012. Raman imaging. Annu. Rev. Anal. Chem. 5, 337–360. https://doi.org/10.1146/annurev-anchem-062011-143152.
Tichota, D.M., Silva, A.C., Lobo, J.M.S., Amaral, M.H., 2014. Design, characterization, and clinical evaluation of argan oil nanostructured lipid carriers to improve skin hydration. Int. J. Nanomedicine 9, 3855–3864. https://doi.org/10.2147/IJN.S64008.
Zhang, X., de Juan, A., Tauler, R., 2015. Multivariate curve resolution applied to hyperspectral imaging analysis of chocolate samples. Appl. Spectrosc. 69, 993–1003. https://doi.org/10.1366/14-07819.
Zhao, Y., Ma, C.-Y., Yuen, S.-N., Phillips, D.L., 2004. Study of succinylated food proteins by Raman spectroscopy. J. Agric. Food Chem. 52, 1815–1823. https://doi.org/10.1021/jf030577a.